



**HAL**  
open science

## Use of Numerical Simulation to Predict Iliac Complications During Placement of an Aortic Stent Graft

Anne Daoudal, Juliette Gindre, Florent Lalys, Moundji Kafi, Claire Dupont, Antoine Lucas, Pascal Haignon, Adrien Kaladji

► **To cite this version:**

Anne Daoudal, Juliette Gindre, Florent Lalys, Moundji Kafi, Claire Dupont, et al.. Use of Numerical Simulation to Predict Iliac Complications During Placement of an Aortic Stent Graft. *Annals of Vascular Surgery*, 2019, 61, pp.291-298. 10.1016/j.avsg.2019.04.035 . hal-02280248

**HAL Id: hal-02280248**

**<https://univ-rennes.hal.science/hal-02280248>**

Submitted on 21 Dec 2021

**HAL** is a multi-disciplinary open access archive for the deposit and dissemination of scientific research documents, whether they are published or not. The documents may come from teaching and research institutions in France or abroad, or from public or private research centers.

L'archive ouverte pluridisciplinaire **HAL**, est destinée au dépôt et à la diffusion de documents scientifiques de niveau recherche, publiés ou non, émanant des établissements d'enseignement et de recherche français ou étrangers, des laboratoires publics ou privés.



Distributed under a Creative Commons Attribution - NonCommercial 4.0 International License

1 **USE OF NUMERICAL SIMULATION TO PREDICT ILIAC**  
2 **COMPLICATIONS DURING PLACEMENT OF AN AORTIC**  
3 **STENT GRAFT**

4 Anne Daoudal<sup>1,2,3</sup> MD, Juliette Gindre<sup>2,3</sup> PhD, Florent Lalys<sup>4</sup> PhD, Moundji Kafi<sup>2,3</sup> MSc,  
5 Claire Dupont<sup>2,3</sup> PhD, Antoine Lucas<sup>1,2,3</sup> MD, Pascal Haigron<sup>2,3</sup> PhD, Adrien Kaladji<sup>1,2,3</sup> MD-  
6 PhD

- 7 1. CHU Rennes, Centre of Cardiothoracic and Vascular surgery, F-35033, Rennes,  
8 France  
9 2. INSERM, U1099, F-35000 Rennes, France  
10 3. University Rennes 1, Signal and Image Processing Laboratory (LTSI), F-35000  
11 Rennes, France  
12 4. Therenva, F-35000, Rennes, France

13 Corresponding author:

14 Adrien Kaladji, Centre of cardiothoracic and vascular surgery, University hospital of Rennes,  
15 F-35033 Rennes, France

16 Article category: original article

17 Short title: Numerical simulation and EVAR procedures

18 Total word count: 2906 words

19

20

## 21 **Abstract**

### 22 **Objective**

23 During endovascular aneurysm repair (EVAR), complex iliac anatomy, is a source of  
24 complications such as unintentional coverage of the hypogastric artery. The aim of our study  
25 was to evaluate ability to predict coverage of the hypogastric artery using a biomechanical  
26 model simulating arterial deformations caused by the delivery system.

### 27 **Methods**

28 The biomechanical model of deformation has been validated by many publications. The  
29 simulations were performed on 38 patients included retrospectively, for a total of 75 iliac  
30 arteries used for the study. On the basis of objective measurements, two groups were formed:  
31 one with "complex" iliac anatomy (n=38 iliac arteries), the other with "simple" iliac anatomy  
32 (n=37 iliac arteries). The simulation enabled measurement of the lengths of the aorta and the  
33 iliac arteries once deformed by the device. Coverage of the hypogastric artery was predicted if  
34 the deformed renal/iliac bifurcation length ( $L_{pre}$ ) was less than the length of the implanted  
35 device ( $L_{stent}$ -measured on the post-operative CT) and non-deformed  $L_{pre}$  was greater than  
36  $L_{stent}$ .

### 37 **Results**

38 Nine (12%) internal iliac arteries were covered unintentionally. Of the coverage attributed to  
39 peri-operative deformations, 1 case (1.3%) occurred with simple anatomy and 6 (8.0%) with  
40 complex anatomy ( $p=0.25$ ). All cases of unintentional coverage were predicted by the  
41 simulation. The simulation predicted hypogastric coverage in 35 cases (46.7%). There were  
42 therefore 26 (34.6%) false positives. The simulation had a sensitivity of 100% and a  
43 specificity of 60.6%. On multivariate analysis, the factors significantly predictive of coverage

44 were the iliac tortuosity index ( $p=0.02$ ), the predicted margin between the termination of the  
45 graft limb and the origin of the hypogastric artery in non-deformed ( $p=0.009$ ) and deformed  
46 ( $p=0.001$ ) anatomy.

#### 47 **Conclusion**

48 Numerical simulation is a sensitive tool for predicting the risk of hypogastric coverage during  
49 EVAR and allows more precise pre-operative sizing. Its specificity is liable to be improved by  
50 using a larger cohort.

51

## 52 INTRODUCTION

53 The widespread uptake of endovascular aneurysm repair (EVAR) for abdominal aortic  
54 aneurysms (AAAs) has given rise to complications specific to this technique. The most well-  
55 known complications are those that occur a while after the surgical procedure, such as  
56 endoleaks. However, there are some complications that can occur during the procedure itself  
57 and are independent of both the technique employed and the surgeon. These are complications  
58 specifically linked to use of stent grafts for treating aortic disease, given that such procedures  
59 attempt to achieve the closest fit possible between the patient's anatomy and the implanted  
60 device. In the last few years, planning tools such as sizing software have advanced  
61 considerably, providing several reconstructions and advanced measurements that permit a  
62 better appreciation of the patient's anatomy and hence optimization of device selection and  
63 the operative strategy to use.

64 Currently, complex anatomy represents the primary challenge for stent graft treatments given  
65 that the size of the eligible patient population is only limited by anatomy. Complex anatomy  
66 is problematic not only for the durability of the seal but also because, during the procedure,  
67 the rigid ancillary tools required to implant the stent graft cause some degree of anatomical  
68 deformation, which can modify the anatomy as perceived, or even precisely measured, before  
69 the procedure and as used to select the device to implant.

70 More specifically, the anatomy of the iliac arteries is highly variable between patients, with  
71 features such as calcification, tortuosity and angulation, which can also be present together.  
72 These arteries are subject to the greatest stress when the stent graft is placed (1) and can give  
73 rise to specific complications such as unintentional coverage of the internal iliac artery — this  
74 complication illustrates the above-mentioned paradox: although pre-operative anatomy is  
75 studied in detail to allow optimal selection of the stent graft, there are no specific tools

76 available with which to predict the behavior of the landing zones, particularly when the stent  
77 graft is definitively delivered.

78 In previous work (2,3), we showed that a numerical finite element simulation enabled  
79 quantification and localization of peri-operative deformations and, after comparing pre-  
80 operative and actual, peri-operative data in 28 patients, we could conclude that we had a  
81 reliable and validated biomechanical model for predicting peri-operative deformation. The  
82 aim of the present study was to evaluate the predictive performance of this model with regard  
83 to unintentional coverage of the internal iliac artery during placement of an aortic stent graft  
84 in the treatment of AAA.

85

## 86 MATERIALS AND METHODS

87 The protocol and informed consent form were approved by the local institutional review board, and all  
88 subjects gave informed consent. This was a retrospective study that compared the anatomy of  
89 iliac arteries defined in two groups: “simple anatomy” vs. “complex anatomy”. Each iliac was  
90 considered as a specific case. Iliac arteries were assigned to one of these two groups on the  
91 basis of their anatomic complexity, as determined using the Society for Vascular Surgery’s  
92 severity grading system (4), described below.

### 93 Analysis of pre-operative CT scan and definition

#### 94 *Measurements used to categorize patients*

95 For each patient, the centerlines of the vasculature were extracted from the pre-operative CT  
96 scan (EndoSize®; Therenva, France). Pre-operative CT data were analyzed and the following  
97 variables were calculated in order to describe pre-operative iliac morphology and to use the  
98 SVS grading system:

- 99 • Iliac tortuosity index: the ratio between the length as measured by the centerline and  
100 the length of the shortest, straight-line path
- 101 • Maximal iliac angulation: measured using a 3D reconstruction
- 102 • Percentage of iliac calcification: determined using a specific measuring tool based on  
103 grayscale values of the Hounsfield scale (5)

104 A severity grade of 0 to 3 was assigned to each calculated value, as per Chaikof’s standards.

#### 105 *Measurements used to test simulation performance*

106 The distance between the lowest renal artery and the ostium of the internal iliac artery  
107 measured using the centerline was called  $L_{pre}$ . This length corresponded to the maximum

108 theoretical deployment zone of the stent graft without coverage of collaterals (renal or internal  
109 iliac arteries).

#### 110 **Analysis of post-operative CT scan**

111 Centerlines were also extracted, with the stent graft in place, from the post-operative CT scan  
112 at 1 month. The first measurement,  $L_{\text{post}}$ , was the length from the lowest renal artery to the  
113 ostium of the internal iliac artery. The second measurement,  $L_{\text{stent}}$ , was the length from the  
114 lowest renal artery to the distal extremity of the graft limbs; this length corresponded to the  
115 length of the stent graft in situ.

#### 116 **Group formation**

117 Patients were included in a non-interventional clinical research protocol, accepted by the  
118 institutional review board of Rennes University Hospital (April 2016) and the French national  
119 data protection agency (CNIL). Patients were included either prospectively (written consent  
120 obtained over a 12-month inclusion period) or retrospectively (a letter was sent to these  
121 patients and they did not provide written objection to retrospective participation in the study).  
122 All patients eligible for endovascular repair of an AAA with a 3rd-generation stent graft could  
123 be included. Patients who died or with intentional coverage of the internal iliac artery, decided  
124 pre-operatively, were excluded. Patients whose CT scans had a slice thickness greater than 1  
125 mm and/or showed heterogeneous arterial enhancement of the aorta and the iliac arteries were  
126 not included. The selection of the stent graft was completely independent of the study, being  
127 entirely at the surgeon's discretion.

128 In order to achieve the same number of patients in both groups, the complex anatomy group  
129 was formed first. These patients had to have a severity grade of 2 or 3 for at least one of the  
130 three measured iliac variables for one or both of their iliac arteries. When a complex anatomy  
131 patient was selected, the next patient (in terms of the procedure date) was selected for the



132 simple anatomy group if they fulfilled the criteria, namely a severity grade of 0 or 1 for the  
133 three measured iliac variables for both iliac arteries.

#### 134 **Numerical simulation**

135 The modeling and simulation method used was described then validated in two previous  
136 publications using peri-operative data from 28 patients.

137 Using the simulation system, it was possible to model the configuration of the vascular tree  
138 deformed by the presence of rigid guide wires and the delivery system (using the patient's  
139 pre-operative CT scan). A simulation was performed for each patient, on the right then on the  
140 left sides. Next, the deformed vascular tree was analyzed in terms of centerline length. The  
141 renal-hypogastric length after insertions of the rigid guide wire and delivery system was  
142 measured on both sides:  $L_{\text{peri}}$ . This length could then be compared to the implanted device in  
143 situ ( $L_{\text{stent}}$ ).

#### 144 *Prediction of residual length*

145 The post-operative residual length (length of uncovered iliac artery) was calculated as the  
146 difference between  $L_{\text{post}}$  and  $L_{\text{stent}}$  and corresponded to the zone of the common iliac artery  
147 not covered by the stent graft. A negative value represented coverage of the internal iliac  
148 artery. The simulated residual length, computed from the model of the aorta deformed by the  
149 presence of the stent graft delivery system and rigid guide wire, was also computed. The post-  
150 operative residual length was analyzed by a statistical predictive model in order to identify the  
151 potential predictive variables from pre-operative anatomical and numerical simulation data.

#### 152 *Prediction of internal iliac coverage*

153 The simulation predicted coverage of the internal iliac on the basis of two essential  
154 conditions: the deformed renal/iliac bifurcation length ( $L_{\text{peri}}$ ) was less than the length of the

155 implanted device ( $L_{\text{stent}}$ ); and  $L_{\text{pre}}$  was greater than  $L_{\text{stent}}$ . If  $L_{\text{pre}}$  was less than  $L_{\text{stent}}$  and  $L_{\text{peri}}$   
156 less than  $L_{\text{stent}}$ , then a sizing error had occurred (Figure 1).

## 157 **Statistical analysis**

158 The first analysis focused on the prediction of the post-operative residual length. Univariate  
159 analyses were used to estimate the influence of pre-operative and simulation parameters.

160 Descriptive analysis and univariate analysis were performed using the  $\chi^2$  test, Fisher's test,  
161 Student's test or Pearson correlation, as appropriate. Parameters with a significance lower  
162 than 0.2 were included in a multivariate analysis performed using multiple linear regression  
163 and an iterative approach to select the best attributes.

164 The second analysis gave rise to a simple strategy for evaluation based on a pre-operative  
165 simulation of risks. By focusing on the presence or absence of coverage (post-operative  
166 residual length  $< 0$ ), the goal was to identify the subgroups of patients at high risk of  
167 complications. The residual lengths predicted by simulating insertion of stiff tools were  
168 directly used for risk stratification. The confusion matrices and ROC curves were thus  
169 calculated using a threshold set at 0 for the estimated lengths.

170 Analyses were performed with the software program R (The R foundation for statistical  
171 computing, 2009).

172

## 173 **RESULTS**

174 The study included 38 patients (mean age:  $77.8 \pm 8.1$  years). Given that one patient had  
175 received an aortomonoiliac stent graft, a total of 75 iliac arteries were studied and simulated,  
176 66 of which (88%) were from men. Thirty-seven and thirty-eight iliac arteries (49.3%) were  
177 assigned to the simple and complex anatomy groups, respectively (Table 1). There were no  
178 significant differences in implanted stent grafts between groups (Table 2,  $p=0.065$ ).

### 179 **Prediction of post-operative residual length**

180 Parameters related to iliac anatomy and patient demographic data were included in the  
181 univariate analysis (Table 3), along with the pre-operative and simulated residual lengths.  
182 From the usual pre-operative anatomical and demographic variables, only the iliac angle score  
183 ( $R = 0.33$ ,  $p = 0.04$ ) could predict the post-operative residual length. The simulated residual  
184 length showed higher predictive value ( $R=0.75$ ,  $p<0.001$ ) than the pre-operative residual  
185 length ( $R = 0.62$ ,  $p < 0.001$ ). In the multivariate analysis, four variables were shown to be  
186 significantly predictive: the pre-operative residual length ( $p=0.009$ ), the simulated residual  
187 length ( $p=0.001$ ), the tortuosity score (0.0224) and the angulation score (0.0587). There was a  
188 high correlation between the simulated and post-operative residual length (Figure 2).

### 189 **Prediction of internal iliac coverage**

190 Among the 75 iliac arteries, there were 9 cases (12%) of unintentional internal iliac coverage,  
191 two of which were due to sizing error. Of the 7 cases attributed to peri-operative deformation,  
192 1 (1.3%) occurred in the simple anatomy group and 6 (8.0%) in the complex anatomy group  
193 ( $p=0.25$ ). After comparison of the real and simulated situations, there was a correspondence  
194 between simulated and real internal iliac coverage (Figure 3). All iliac arteries covered  
195 accidentally were also covered in the simulation. The sensitivity of the simulation was 100%.

196 The simulation predicted internal iliac coverage in 35 cases (46.7%). Hence there were 26  
197 (34.6%) patients who had internal iliac coverage in the simulation but not in reality. The  
198 specificity of the simulation was 60.6%. Coverage of the internal iliac artery (yes/no) via the  
199 difference in the residual length after insertion of the delivery system/length of the stent graft  
200 in situ ( $L_{\text{post}}$ ) was predicted with an area under the curve of 0.91 (Figure 4).

201

## 202 **DISCUSSION**

203 In this article, we describe the use of simulation to predict a complication during the surgical  
204 procedure. The simulation models deformable anatomy (a property of soft tissues such as  
205 arteries) and its interactions with rigid materials. The current version of the numerical model  
206 focuses on the consequences of deformation during the aortic endovascular procedure, which  
207 are two-fold. First, by reducing arterial length, deformations have an impact on calibration.  
208 This illustrates the paradox of current practice whereby planning is based on an arterial  
209 volume that has different dimensions when the stent graft is deployed. This paradox is a  
210 source of complication and error. The exact quantification of deformation-related shortening  
211 is difficult and not based on statistical data. Coverage of internal iliac arteries is responsible  
212 for buttock claudication and even pelvic ischemia (6–9) so must be avoided at all costs, but it  
213 presents enormous planning challenges in complex anatomy. Such coverage could be related  
214 to a sizing error, as occurred with two patients included in the present study, but it is more  
215 often related to deformations of the aortoiliac vasculature caused by insertion of rigid material  
216 such as the rigid guide wire and the stent graft delivery system.

217 In our study, we set ourselves the task of predicting the residual length of the common iliac  
218 artery, i.e. the length not covered by the stent graft, because it is one of the variables that  
219 every surgeon intuitively attempts to control for when choosing the length of the stent graft to  
220 implant. To achieve a realistic model, we decided to determine the length of the stent graft on  
221 the basis of the post-operative CT scan rather than using the value in the catalog. There is  
222 indeed a difference between catalog length and in situ length. Our study showed that no single  
223 anatomical variable is able to predict the post-operative residual length without the aid of  
224 simulation. The most predictive variable was the residual margin between the extremity of the  
225 graft limb and the ostium of the internal iliac, in an aorta deformed by the stent graft delivery

226 system. This result highlights the utility of simulation when planning EVAR. Finally, in this  
227 study of a highly specific clinical complication — coverage of the internal iliac — the results  
228 showed that simulation alone is capable of predicting this risk with a robust model (ROC  
229 curve). The clinical relevance of this study was to predict coverage of the internal iliac artery.  
230 All cases of unintentional coverage were predicted by the numerical simulation. In clinical  
231 practice, this simulation model could play an important role in reducing iliac complications  
232 during EVAR procedures.

233 Whittaker *et al.* (10) proposed an algorithm to predict the length of the stent graft modified  
234 during the EVAR procedure; however their model was based on pre- and post-operative CT  
235 data, whereas peri-operative data are more precise for preventing and predicting peri-  
236 operative complications. Iliac tortuosity is known to be a source of complications during or  
237 after EVAR and represents a difficult aspect of the procedure. In our previous works (2,3), we  
238 showed that the reliability of our model extended to complex cases. Conformation of aortic  
239 stent grafts has already been studied by comparing *in vitro* or *in vivo* models with a numerical  
240 simulation (11–13), and it was shown that stent graft behavior could be anticipated from the  
241 anatomy, notably in cases of complex anatomy.

242 The second consequence of deformation during EVAR procedures concerns the precision of  
243 rigid registration in fusion imaging. It is currently accepted in several articles (1,14) that  
244 deformation represents the leading source of registration error when the pre-operative CT  
245 scan is laid over the 2D fluoroscopic image. It is the primary factor limiting fusion imaging.  
246 With the aid of a numerical deformation model, the precision of fusion can be improved,  
247 helping to achieve precise positioning of the graft limbs (Figure 5).

248 Another approach to gain precision would be to perform intra-operative length measurements,  
249 using for instance a calibrated pigtail catheter after the introduction of stiff guide-wire, and  
250 integrate these data into new predictive models or refine previous ones.

251 Our study has several limitations. The number of patients is small; it is probable that a greater  
252 number of patients would improve the robustness of the model (its specificity, among other  
253 aspects). The incidence of complex anatomy was low and we were not able to include more  
254 patients from our center fulfilling the study criteria. There may also be a selection bias, as  
255 patients with too complex iliac anatomy could have undergone open surgery. However, at our  
256 center, since the emergence of 3rd-generation stent grafts, iliac access has not been a  
257 contraindication to EVAR, with the exclusion of iliac occlusion. At our center,  
258 contraindications to EVAR only concern the proximal neck (length < 10 mm). Improvements  
259 in the profile of stent grafts have allowed procedures with stenosed and tortuous access  
260 vessels, sometimes with additional steps such as paving and cracking when applicable. This is  
261 why we did not retrospectively include patients at our center treated with 2nd-generation stent  
262 grafts. Complex anatomy therefore represents a veritable clinical challenge. Obviously, there  
263 are solutions for better appreciating deformations, for example taking peri-operative iliac  
264 measurements using graduated markings on the rigid guide wire, but this technique carries  
265 with it the risk of parallax error, which is greater with tortuous iliac arteries.

266 One unresolved issue, whose existence provides the impetus for us to continue working on  
267 numerical simulation, is the behavior of the iliac artery after delivery of the stent graft and  
268 withdrawal of the rigid guide wire. In our practice, we have observed that sometimes the  
269 anatomy (even sometimes tortuous anatomy) reverts to its initial form and sometimes it does  
270 not. This behavior is multifactorial and probably difficult to predict because it also depends on  
271 the implanted stent graft and its biomechanical characteristics. Our simulation model should  
272 therefore simulate delivery of the stent graft, and take into account the overlapping of

273 different modules and the different brands of stent graft. Reaching this point requires a  
274 significant technical and scientific leap forward. This is why we initially decided that data  
275 from deformation by one guide wire and one delivery system were sufficient to develop a  
276 reliable, robust and precise tool for predicting peri-operative arterial behavior. Other  
277 applications under study include the displacement of ostia of renal and gastrointestinal arteries  
278 during placement of a fenestrated stent graft, which poses problems, not only for sizing, but  
279 also for peri-operative positioning of the stent graft and catheterization. Transfer to other  
280 centers remains a problem. However it is possible to simplify the model without sacrificing  
281 precision so that it becomes less time-consuming to use and can be integrated into sizing  
282 programs used routinely in clinical practice.

## 283 **CONCLUSION**

284 Evaluation of surgical risk is a constant concern for surgeons. Numerical simulation provides  
285 precise information about arterial biomechanical behavior during implantation of an aortic  
286 stent graft. Complex anatomy is associated with a higher incidence of peri-operative iliac  
287 complications due to deformation. Simulation models deformations and could provide  
288 quantitative information that would reduce the risk of complications.

## 289 **Acknowledgments**

290 This work has been partially conducted in the experimental platform TherA-Image (Rennes,  
291 France) supported by Europe FEDER. This study has been partially supported by the French  
292 National Research Agency (ANR) in the context of the Endosim project (grant n° ANR-13-  
293 TECS-0012).



294 **REFERENCES**

- 295 1. Kaladji A, Dumenil A, Castro M, Cardon A, Becquemin J-P. Prediction of deformations  
296 during endovascular aortic aneurysm repair using finite element simulation. *Comput Med*  
297 *Imaging Graph.* 2013;
- 298 2. Gindre J, Bel-Brunon A, Rochette M, Lucas A, Kaladji A, Haigron P, et al. Patient-  
299 Specific Finite-Element Simulation of the Insertion of Guidewire During an EVAR Procedure:  
300 Guidewire Position Prediction Validation on 28 Cases. *IEEE Trans Biomed Eng.* mai  
301 2017;64(5):1057-66.
- 302 3. Gindre J, Bel-Brunon A, Kaladji A, Duménil A, Rochette M, Lucas A, et al. Finite  
303 element simulation of the insertion of guidewires during an EVAR procedure: example of a  
304 complex patient case, a first step toward patient-specific parameterized models. *Int J Numer*  
305 *Methods Biomed Eng.* juill 2015;31(7):e02716.
- 306 4. Chaikof EL, Fillinger MF, Matsumura JS, Rutherford RB, White GH, Blankensteijn JD, et  
307 al. Identifying and grading factors that modify the outcome of endovascular aortic aneurysm  
308 repair. *J Vasc Surg.* mai 2002;35(5):1061-6.
- 309 5. Kaladji A, Vent P., Danvin A, Chaillou P, Costargent A, Guyomarch B, et al. Impact of  
310 Vascular Calcifications on Long Femoropopliteal Stenting Outcomes. *Ann Vasc Surg.* févr  
311 2018;48:170-8.
- 312 6. Jean-Baptiste E, Brizzi S, Bartoli MA, Sadaghianloo N, Baqué J, Magnan P-E, et al.  
313 Pelvic ischemia and quality of life scores after interventional occlusion of the hypogastric  
314 artery in patients undergoing endovascular aortic aneurysm repair. *J Vasc Surg.* juill  
315 2014;60(1):40-49.e1.
- 316 7. Pirvu A, Gallet N, Perou S, Thony F, Magne J-L. Midterm results of internal iliac artery  
317 aneurysm embolization. *JMV-J Médecine Vasc.* mai 2017;42(3):157-61.
- 318 8. Fujioka S, Hosaka S, Morimura H, Chen K, Wang ZC, Toguchi K, et al. Outcomes of  
319 Extended Endovascular Aortic Repair for Aorto-Iliac Aneurysm with Internal Iliac Artery  
320 Occlusion. *Ann Vasc Dis.* 2017;10(4):359-63.
- 321 9. Bosanquet DC, Wilcox C, Whitehurst L, Cox A, Williams IM, Twine CP, et al. Systematic  
322 Review and Meta-analysis of the Effect of Internal Iliac Artery Exclusion for Patients  
323 Undergoing EVAR. *Eur J Vasc Endovasc Surg.* avr 2017;53(4):534-48.
- 324 10. Whittaker DR, Dwyer J, Fillinger MF. Prediction of altered endograft path during  
325 endovascular abdominal aortic aneurysm repair with the Gore Excluder. *J Vasc Surg.* avr  
326 2005;41(4):575-83.

- 327 11. De Bock S, Iannaccone F, De Santis G, De Beule M. Virtual evaluation of stent graft  
328 deployment: A validated modeling and simulation study. *J Mech Behav Biomed Mater.* 2012;
- 329 12. Perrin D, Badel P, Orgeas L. Patient specific simulation of endovascular repair surgery  
330 with tortuous aneurysms requiring flexible stentgrafts.pdf. *journal of the mechanical*  
331 *behavior of biomedical materials*; 2016.
- 332 13. Perrin D, Badel P, Orgeas L. Patient specific numerical simulation of stentgraft  
333 deployment validation on three clinical cases. *journal of the mechanical behavior of*  
334 *biomedical materials*; 2016.
- 335 14. Duménil A, Kaladji A, Castro M, Göksu C, Lucas A, Haigron P. A versatile intensity-  
336 based 3D/2D rigid registration compatible with mobile C-arm for endovascular treatment of  
337 abdominal aortic aneurysm. *Int J Comput Assist Radiol Surg.* sept 2016;11(9):1713-29.
- 338
- 339

340 **Legends for figures**

341 Figure 1: Definition of prediction of coverage.  $L_{pre}$  is the renal-iliac length without  
342 deformation,  $L_{peri}$  is the same length adjusted by simulation and after deformation, and  
343  $L_{stent}$  is the length of the stentgraft in situ measured on postoperative CT scan.

344 Figure 2

345 Prediction of the post-operative (real) residual length: calibration plot

346 Figure 3

347 Distribution of false positive (FP), true positive (TP), false negative (FN) and true negative  
348 (TN), based on the post-operative (real) and simulated (predicted) residual length.

349 Figure 4

350 ROC curve using logistic regression

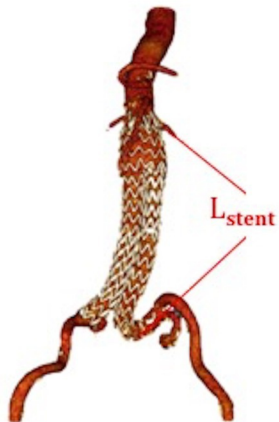
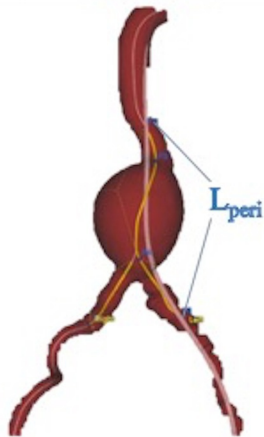
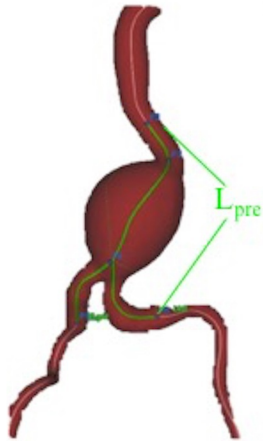
351 Figure 5

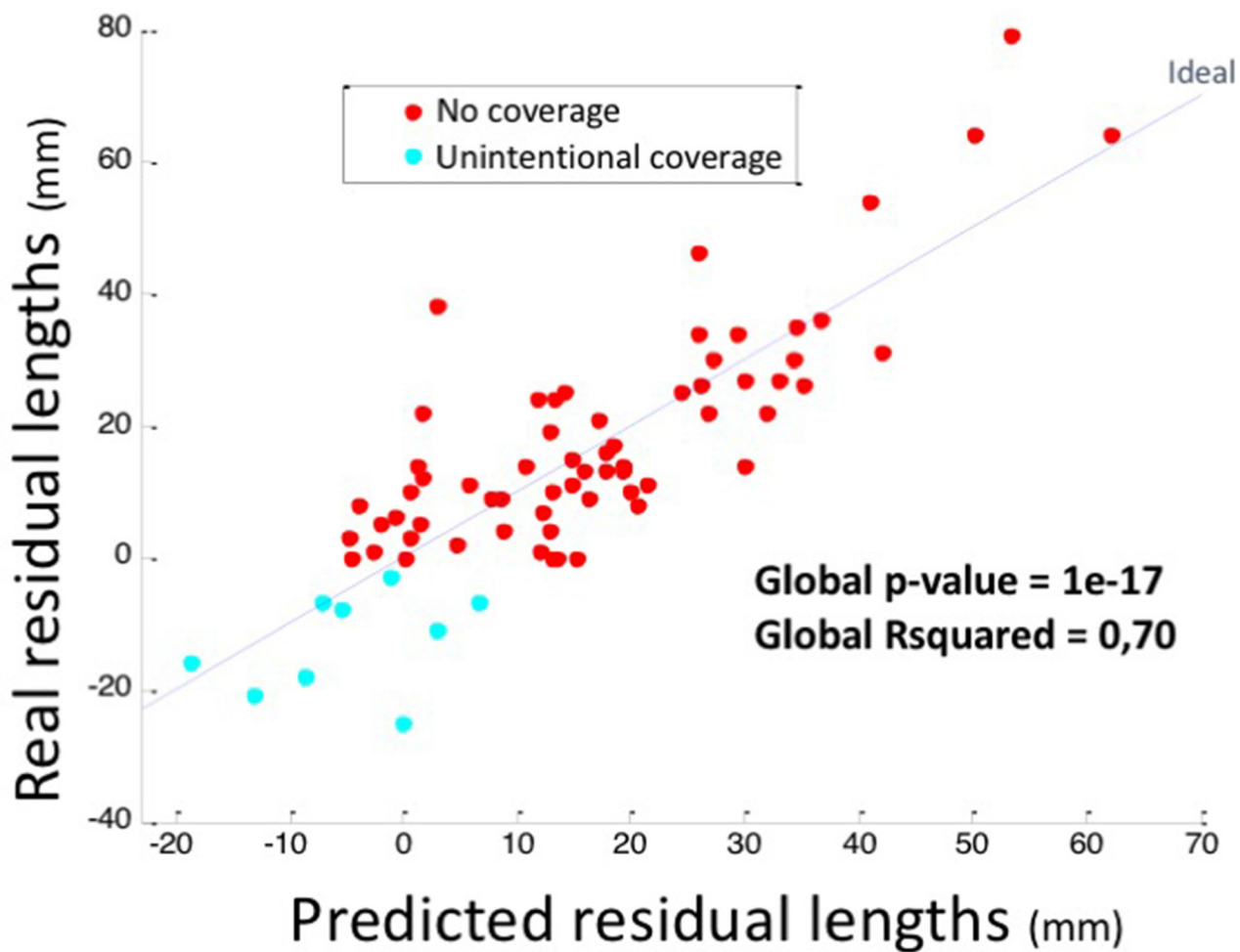
352 Application of simulation in endovascular navigation for fusion imaging. Fluoroscopic image  
353 with the fusion of the 3D preoperative anatomy without deformation (A) and the same image  
354 with deformation

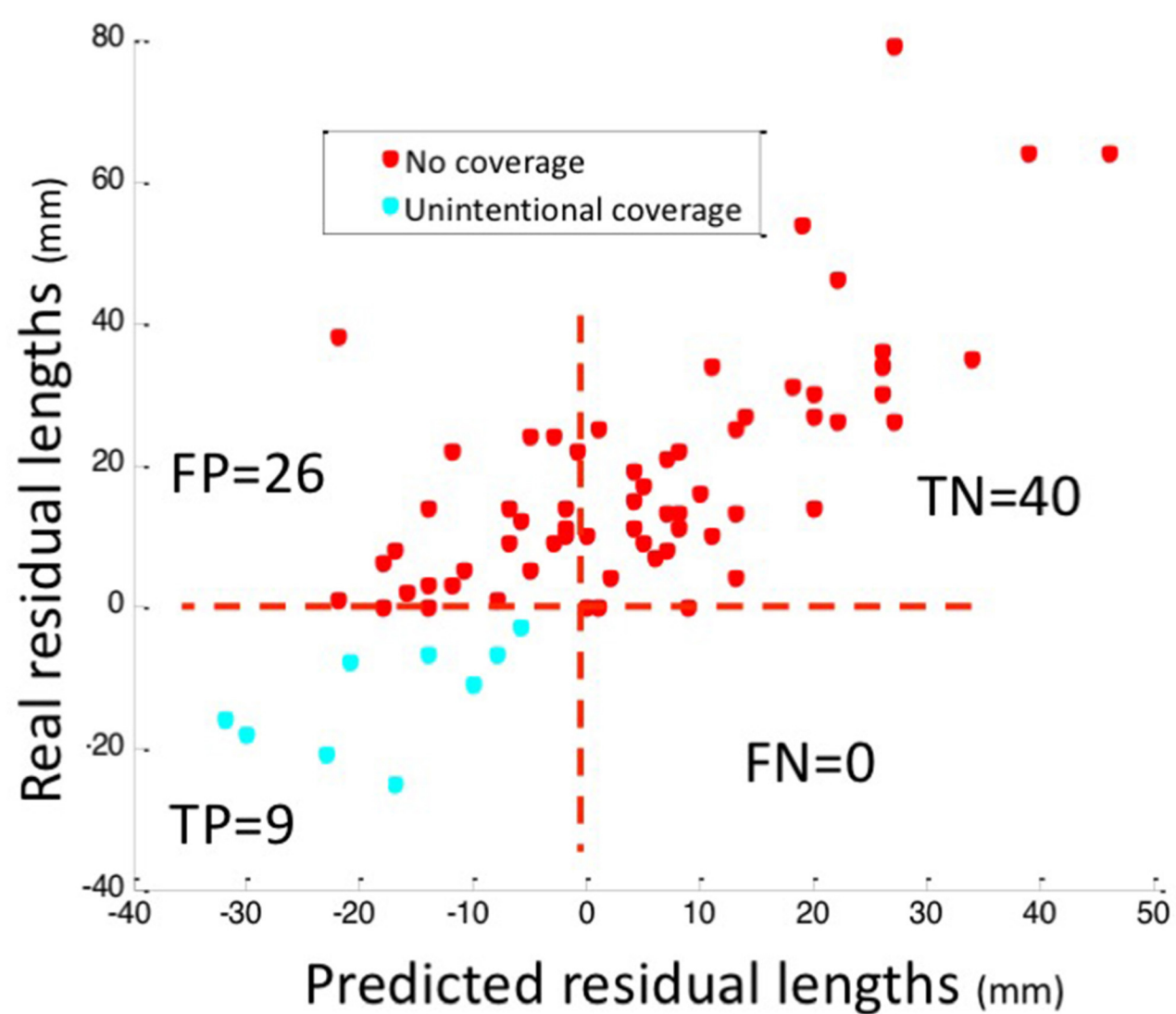
355

If  $L_{stent} > L_{peri}$  AND if  $L_{stent} < L_{pre}$  = prediction of coverage

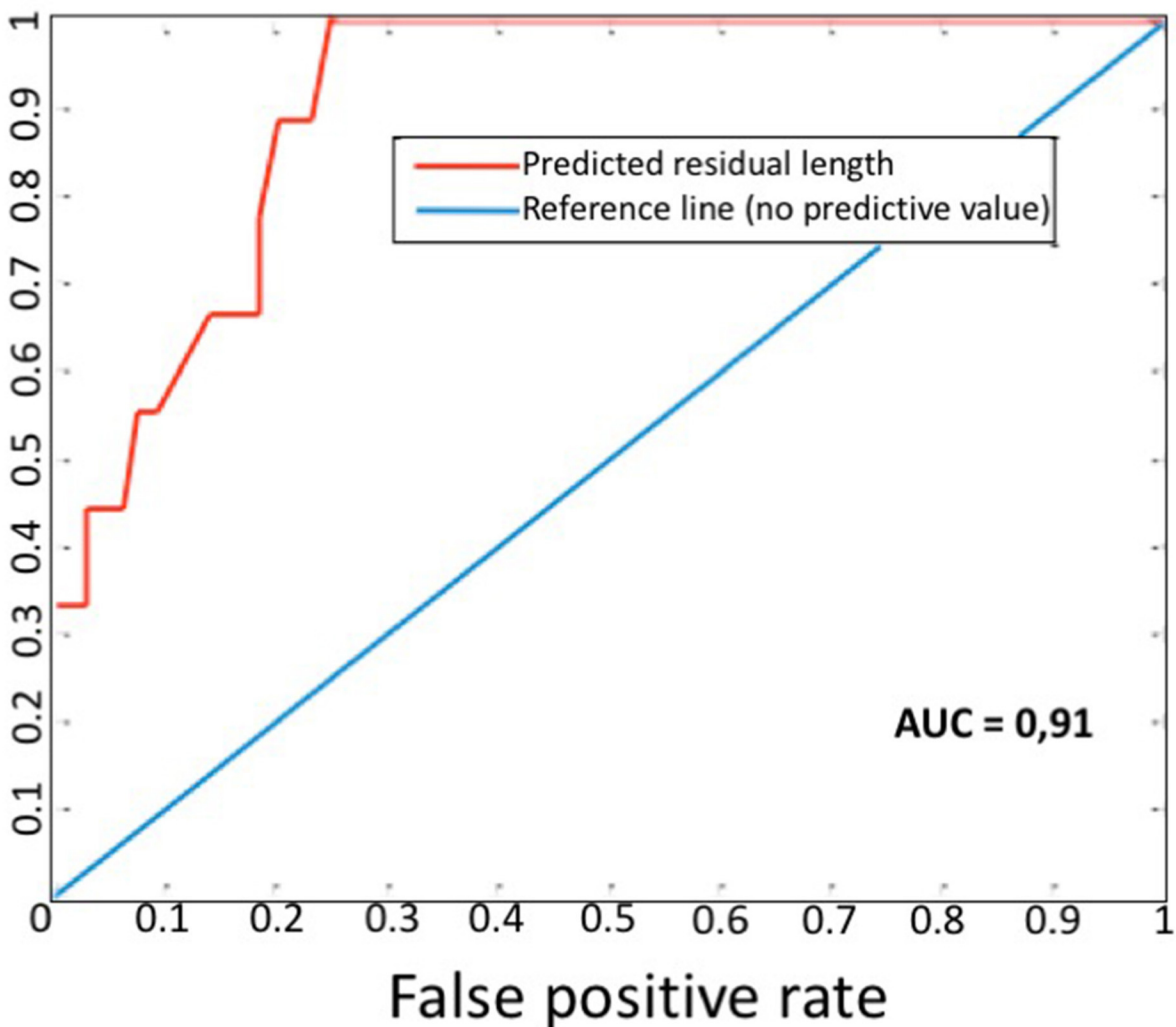
If  $L_{stent} > L_{pre}$  = sizing error







True positive rate



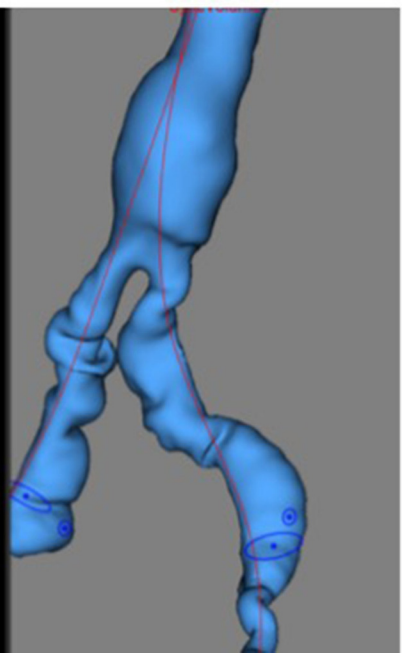
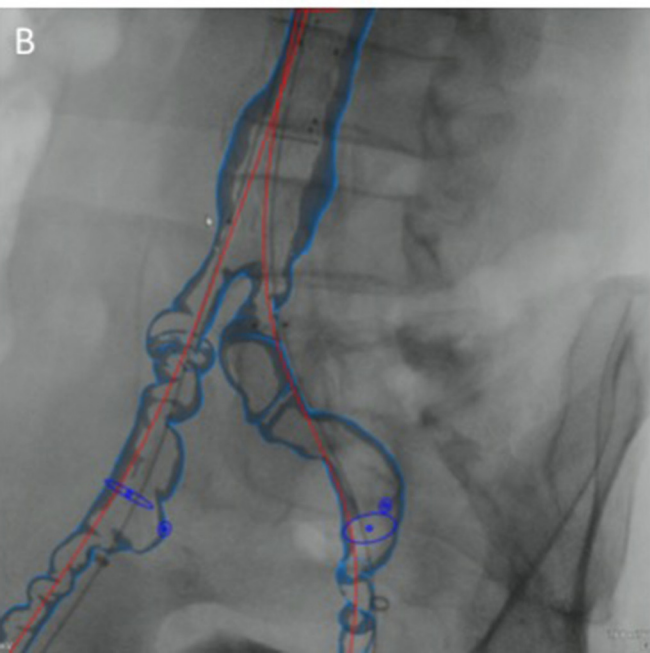
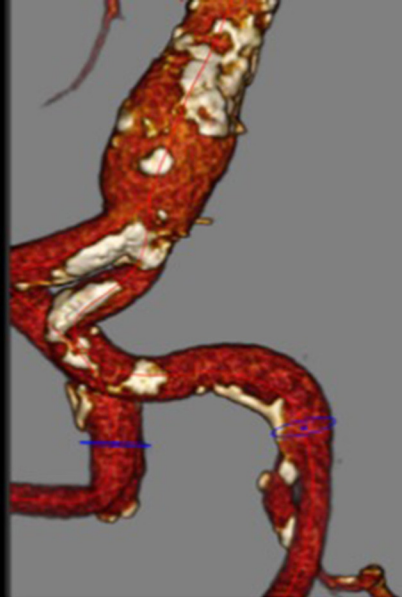
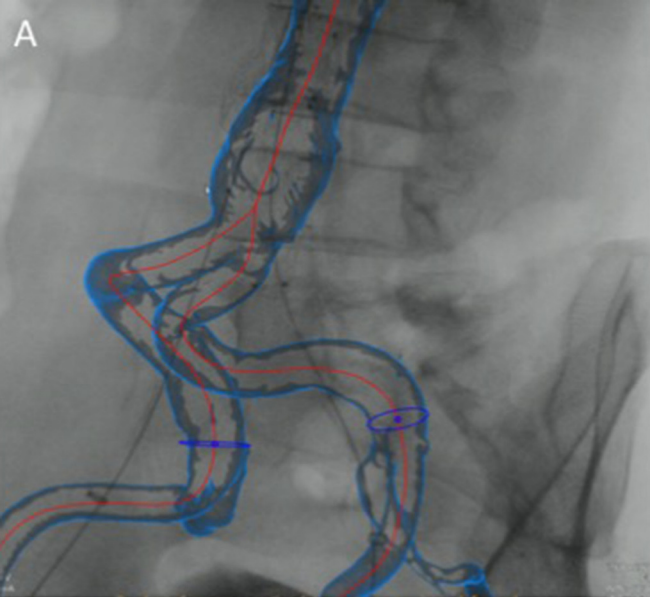




**Table 1:** Descriptive analysis: comparison of demographic and anatomical parameters between groups

	Simple anatomy (n=37)	Complex anatomy (n=38)	<i>p</i>
<b>Pre-operative aorto-iliac length (cm, mean ± SD)</b>	176.9 ± 17.9	194.6 ± 21.2	<0.01
<b>Age (Years, mean ± SD )</b>	77.1 ± 8.2	77.8 ± 8.1	0.45
<b>Sex (male, number (%))</b>	31 (83,8%)	35 (92,1%)	0.15
<b>Iliac tortuosity index (mean ± SD)</b>	1.34 ± 0.09	1.54 ± 0.17	<0.01
<b>Tortuosity score (number (%))</b>			<0.01
0 (index<1.25)	6 (16.2%)	2 (5.3%)	
1 (1.25<index<1.5)	31 (83.8%)	10 (26.3%)	
2 (1.5<index<1.6)	0 (0%)	14 (36.8%)	
3 (index>1.6)	0 (0%)	12 (31.6%)	
<b>Maximal iliac angle (mean ± SD)</b>	142 ± 13.27	107.58 ± 19.83	<0.01
<b>Iliac angle score (number (%))</b>			<0.01
0 (160°-180°)	3 (8,1%)	0 (0%)	
1 (121°-159°)	34 (91.9%)	11 (28.9%)	
2 (90°-120°)	0 (0%)	19 (50%)	
3 (<120°)	0 (0%)	8 (21%)	
<b>Iliac calcifications (mean ± SD)</b>	20% ± 0.15	16% ± 0.14	<0.01
<b>Calcification score (number (%))</b>			<0.01
0 (none)	0 (0%)	4 (10.5%)	
1 (<25% vessel length)	28 (75.7%)	26 (68.4%)	
2 (25% - 50% vessel length )	7 (18.9%)	8 (21.1%)	
3 (>50% vessel length)	2 (5.4%)	0 (0%)	

**Table 2:** Repartition of the implanted stentgrafts according to groups

	Cook - Zenith alpha	Endologix - AFX	Gore - Excluder C3	Medtronic - Endurant II
<b>Simple anatomy</b>	10	4	6	17
<b>Complex anatomy</b>	12	3	0	23
<b>Total</b>	22	7	6	40

**Table 3:** Prediction of the post-operative residual length: univariate analysis.

	<b>total (n=75)</b>	<i>p</i>
<b>Pre-operative aorto-iliac length (cm, mean ± SD)</b>	185.9 ± 21.4	0.06
<b>Age (Years, mean ± SD )</b>	77.4 ± 8.1	0.57
<b>Sex (male, number (%))</b>	66 (88%)	0.34
<b>Iliac tortuosity index (mean ± SD)</b>	1.44 ± 0.17	0.73
<b>Tortuosity score (number (%))</b>		0.09
0 (index<1.25)	8 (10.7%)	
1 (1.25<index<1.5)	41 (54.7)	
2 (1.5<index<1.6)	14 (18.7%)	
3 (index>1.6)	12 (16%)	
<b>Maximal iliac angle (mean ± SD)</b>	125 ± 24.27	0.12
<b>Iliac angle score (number (%))</b>		0.04
0 (160°-180°)	3 (4%)	
1 (121°-159°)	45 (60%)	
2 (90°-120°)	19 (25.3%)	
3 (<120°)	8 (10.7%)	
<b>Iliac calcifications (mean ± SD)</b>	18% ± 0.15	0.51
<b>Calcification score (number (%))</b>		0.35
0 (none)	4 (5.3%)	
1 (<25% vessel length)	54 (72%)	
2 (25% - 50% vessel length)	15 (20%)	
3 (>50% vessel length)	2 (2.7%)	
<b>Pre-operative residual length*</b>	24.5 ± 19.9	<0.01
<b>Simulated residual length**</b>	0.5 ± 17.9	<0.01

\* Difference between Lpre and Lstent

\*\* Difference between Lperi and Lstent